ELSEVIER

Chemical Engineering Journal 69 (1998) 1–5

Chemical Engineering Journal

A study of the morphology of the goethite crystallization process

Tingjie Wang, Yong Jin *, Zhanwen Wang, Zhiqing Yu

Department of Chemical Engineering, Tsinghua University, Beijing 100084, China

Received 12 April 1997; revised 29 July 1997; accepted 22 August 1997

Abstract

Experiments were performed in 1.5- and 150-l reactors to investigate the growth process of needle-like goethite crystals under alkaline conditions. From an analysis of the transmission electron micrographs of the crystal samples during the reaction process, the nucleation and growth processes of the crystal grains were examined. Evidence shows that the nucleation of α-FeOOH crystals occurs both on the surface of the $Fe(OH)_2$ crystal grains and in the bulk liquid, depending on the local concentration of the α-FeOOH molecules. The statistical results of the particle size show that the average length and width are both basically proportional to $R^{1/3}$. The crystals grow in a similar manner and the size distribution is held roughly constant during the crystal-growth process. The influence of the oxidation rate during the early period of the reaction process on the parameters of the final crystal grains was examined. The average aspect ratio of the final α-FeOOH grains increases with the decreasing of the oxidation rate in the early period. The particle size changes as a result of aging under certain pH and temperature conditions. © 1998 Elsevier Science S.A.

Keywords: Goethite; Crystal nucleation; Crystal growth; Magnetic recording medium; Oxidation

1. Introduction

The needle-like magnetic recording medium of γ-Fe_2O_3 can be produced through the reduction and oxidation of needle-like goethite α-FeOOH crystals. Two steps occur: α-FeOOH formation:

$$Fe^{2+} + 2OH^- \rightarrow Fe(OH)_2(s) \quad (1)$$

$$4Fe(OH)_2 + O_2 \rightarrow 4\alpha\text{-FeOOH}(s) + 2H_2O \quad (2)$$

α-FeOOH heat treatment:

$$2\alpha\text{-FeOOH} \rightarrow \alpha\text{-}Fe_2O_3 + H_2O \quad (3)$$

$$3\alpha\text{-}Fe_2O_3 + H_2 \rightarrow 2Fe_3O_4 + H_2O \quad (4)$$

$$4Fe_3O_4 + O_2 \rightarrow 6\gamma\text{-}Fe_2O_3 \quad (5)$$

The manufacture of α-FeOOH is a key step in the production process of the recording medium, because its quality essentially affects the magnetic powder characteristics. In this paper, we study the nucleation and growth processes of needle-like goethite crystals.

* Corresponding author. Tel.: +86-10-62785464; fax: +86-10-62770304; e-mail: wf.dce@mail.tsinghua.edu.cn

PII S1385-8947(97)00104-6

2. Experimental details

The experiments were carried out in a reactor with an inside diameter (i.d.) of 500 mm and a volume of 150 l. The ratio of alkali to ferrous ions Fe^{2+} ($NaOH/2FeSO_4$) was 2.4, and the reaction temperature was controlled at ~37–39°C. $FeSO_4$ solution was mixed with the alkali solution. The reaction rate was controlled by adjusting the gas flux, and the oxidation rate was deliberately controlled according to a designed curve. The concentration of ferrous ions was measured periodically to monitor the reaction rate during the process.

In order to study the nucleation and growth processes of α-FeOOH crystals, reactants were sampled from the reactor at regular time intervals. The sampled reactants were treated in a certain volume of dilute sulphuric acid solution (pH 1.5). Because the equilibrium constant for $Fe(OH)_2$ K_{sp}, is 10^{-14} and that for α-FeOOH is 10^{-44} [1], $Fe(OH)_2$ was dissolved, but there was little influence on α-FeOOH. Nitrogen gas was injected into the dilute acid solution to remove oxygen before sampling. In the final powder samples, $Fe(OH)_2$ particles were washed off, and only α-FeOOH remained. The size and aspect ratio of the α-FeOOH crystals were measured by transmission electron microscopy (TEM) with ~70–140 counted particles. The statistical reliability of sampling is 95% by F-function test.

3. Experimental results and discussion

3.1. Nucleation

Various viewpoints exist on the mechanism of the nucleation and growth of α-FeOOH crystals under alkaline conditions. Feitknecht [2] reported that α-FeOOH crystals are formed by the surface oxidation of $Fe(OH)_2$FeOOH. Misawa et al. [3] proposed that $Fe(OH)_2$ dissolves into solution as $Fe(OH)_3^-$, followed by reaction with dissolved oxygen to form α-FeOOH crystals. Bernal et al. [4] reported that the nucleation and growth processes of α-FeOOH crystals are the result of the oxidation and precipitation of ionized Fe^{2+} in solution from $Fe(OH)_2$. Sada et al. [5] reported that $Fe(OH)_2$ is ionized to $HFeO_2^-$, which is oxidized to $(Fe_2(OH)_3)_n^{3n+}$; finally, α-FeOOH crystals are formed, mainly in the bulk liquid phase, through the hydrolysis of $(Fe_2(OH)_3)_n^{3n+}$. Du and Lou [6] proposed that Fe^{2+} is ionized from $Fe(OH)_2$, and then oxidized to give α-FeOOH at the gas–liquid interface. Gu et al. [7] reported that the nucleation of α-FeOOH occurs on the crystal surface of the $Fe(OH)_2$, and the growth of the α-FeOOH crystal grains is the result of the coagulation of the crystallite.

Due to the complexity of the α-FeOOH crystallization process, the mechanisms of nucleation and growth are not fully understood and require further investigation. This was the purpose of this study.

Fig. 1 shows the transmission micrographs of α-FeOOH obtained from a suspension treated with dilute acid solution. $Fe(OH)_2$ in the suspension is a hexagonal tabular crystal and α-FeOOH is a needle-like crystal. In Fig. 1a, a hexagonal hole is formed by α-FeOOH crystal columns whose borders show traces of dissolution. The diameter of the hole in the figure is about 0.05 μm which is close to the diameter of the $Fe(OH)_2$ crystal reported by Sada et al. [5]. This shows that the hexagonal hole is not formed by six α-FeOOH crystal columns piled together, but is left after a crystal of $Fe(OH)_2$ has been dissolved in dilute sulphuric acid solution from a crystal cluster. From this figure the adjacent α-FeOOH crystals have angles of 60°. On the basis of this evidence, it can be deduced that the α-FeOOH crystal nucleates on the surface of the $Fe(OH)_2$ crystal grains, and grows along the border of the hexagon. As the reaction proceeds, the growing α-FeOOH crystal grains disengage from the surface of $Fe(OH)_2$ naturally or as a result of friction and shear. The disengaged crystal grains continue to grow.

Therefore the size and size distribution of the $Fe(OH)_2$ grains before oxidation have a certain influence on the α-FeOOH nucleation and growth processes. The uniformity of the $Fe(OH)_2$ size distribution can be improved by controlling the micromixing conditions between Fe^{2+} and OH^-. Thus the uniformity of the α-FeOOH crystals can also be improved.

Two kinds of crystals can be seen from an examination of the crystal micrographs during the reaction process. One is a large crystal with some corrosion traces and an aspect ratio between 6 and 12. It originates on the surface of the $Fe(OH)_2$ crystals as discussed above. The other is an integrated, long, thin crystal without corrosion traces, with an aspect ratio larger than 15 (Fig. 1b). This kind of crystal nucleation occurs in the bulk liquid phase due to the high supersaturation of the local α-FeOOH concentration. It takes place when the oxidation rate is very rapid for a period of time or instantaneously during the reaction process. The fine nucleus remains, without dissolution when it is larger than a critical nucleus size. Crystallization competes with nucleation for α-FeOOH molecules. Crystallization possesses the advantage of having an already existing large nucleus. Nucleation in the bulk can be avoided by appropriate control of the oxidation rate and by intensifying micromixing in the bulk liquid [8]. Therefore the control of the reaction rate during the crystal-growth process is very important for obtaining a uniform-size distribution of the final product.

Fig. 2 shows the conversion curves. During the reaction process, the fluid viscosity in the reactor increases as the reaction proceeds. The gas flux must be controlled carefully to reduce the reaction rate especially at the beginning, due to the low viscosity. The basic concept of designing the conversion curves is to control the nucleation at the beginning

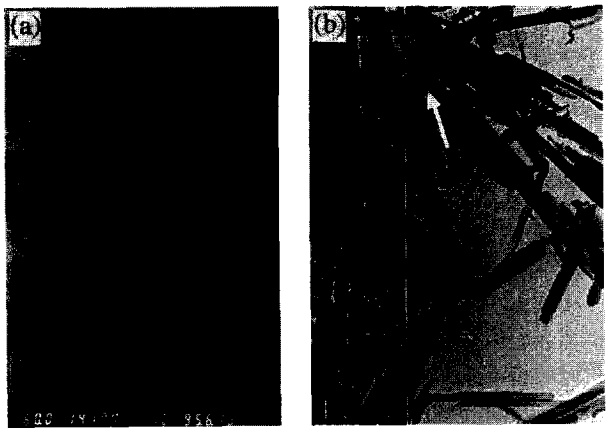

Fig. 1. Transmission electron micrographs of α-FeOOH crystal grains showing nucleation: (a) test 1, $C_0 = 0.4$ mol l^{-1}, $R = 32\%$, $k = 80\,000$; (b) test 2, $C_0 = 0.32$ mol l^{-1}, $R = 5\%$, $k = 83\,000$.

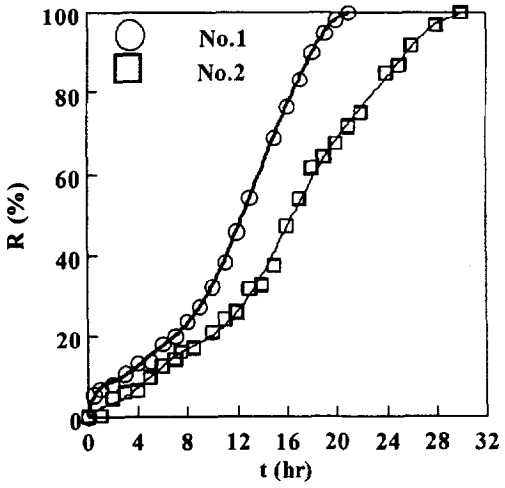

Fig. 2. Conversion control during the reaction process.

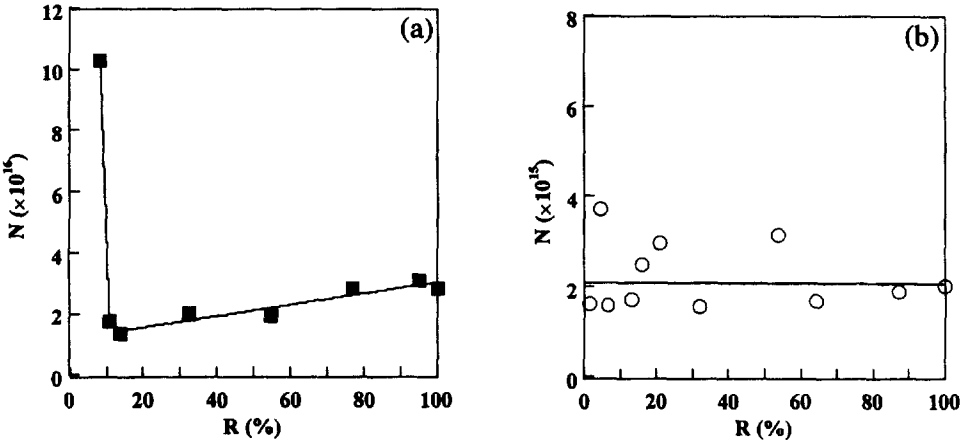

Fig. 3. Number of α-FeOOH crystals per unit volume (1) of the reactant vs conversion degree: (a) test 1, (b) test 2.

and the crystal growth at the end in order to maintain a uniform crystal size.

α-FeOOH crystals have a square cylindrical shape. The average volume can be calculated according to the average length and width of the crystal grains. The number of α-FeOOH crystal grains at a certain degree of conversion in a unit volume can be approximately determined by

$$N = C_0 MR/(\rho V) \quad (6)$$

where C_0 is 0.40 mol l^{-1} for test 1 and 0.32 mol l^{-1} for test 2, $M = 89$ g mol^{-1}, $\rho = 4200$ g l^{-1}, R is the conversion and V is the average volume of the crystal grains.

Fig. 3 shows that the amount of α-FeOOH crystal grains per unit volume (1) changes with the degree of conversion. In test 1, a large amount of crystal grains form at the beginning; the number then sharply decreases because of coagulation and dissolution over 2–3 h. This results from the high oxidation rate at the beginning and the lower oxidation rate thereafter (see Fig. 2). As the reaction proceeds, the number of crystal grains in the reactor increases with increasing degree of conversion. This shows that nucleation occurs in the latter process in test 1. In test 2, however, the number of crystal grains is maintained roughly constant, although there is some fluctuation. This shows that crystallization controls nucleation through competition in test 2. It can be seen in Fig. 2 that the oxidation in test 1 is faster than that in test 2, and the initial concentration of ferrous ions in test 1 is higher than that in test 2. Locally high supersaturation of α-FeOOH molecules occurs easily in test 1, which may explain the nucleation difference between test 1 and test 2.

3.2. Growing process

During the reaction process, samples were taken at different degrees of conversion from the beginning of oxidation. Samples within the first 2 h were not available, since the crystal grains were completely dissolved in the dilute acid solution because of the large specific surface area. Figs. 4 and 5 shows the changing trends of the average size and aspect ratio with the degree of conversion in test 1 and test 2.

It can be seen from Figs. 4 and 5 that the crystals grow rapidly during the early oxidation period. The average length and width of the crystals increase with increasing degree of conversion, following similar changing laws. The average length and width are basically proportional to $R^{1/3}$. The aspect ratio remains essentially constant during the reaction process. The crystal grains grow in a similar manner. The axial growth velocity is faster than the radial growth velocity. Fig. 5 shows that the particle size in test 2 is larger than that in test 1. It also shows that crystal growth controls the process in test 2.

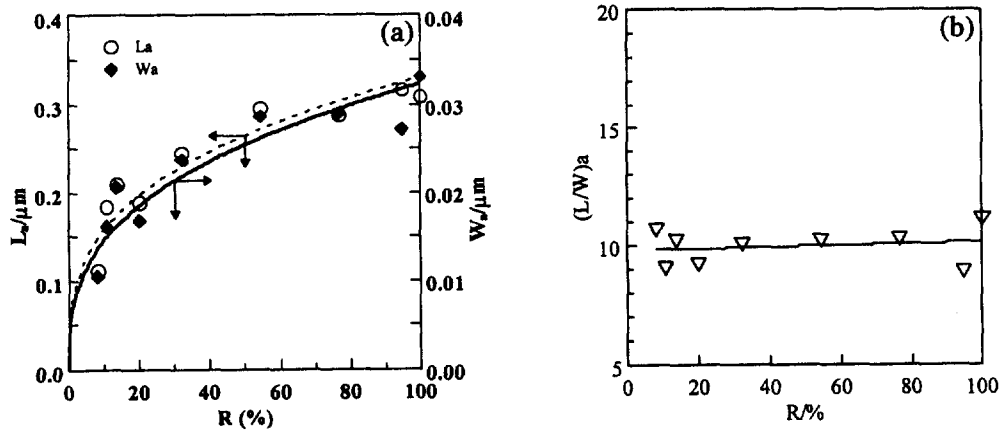

Fig. 4. Average length, width and aspect ratio vs conversion degree (test 1).

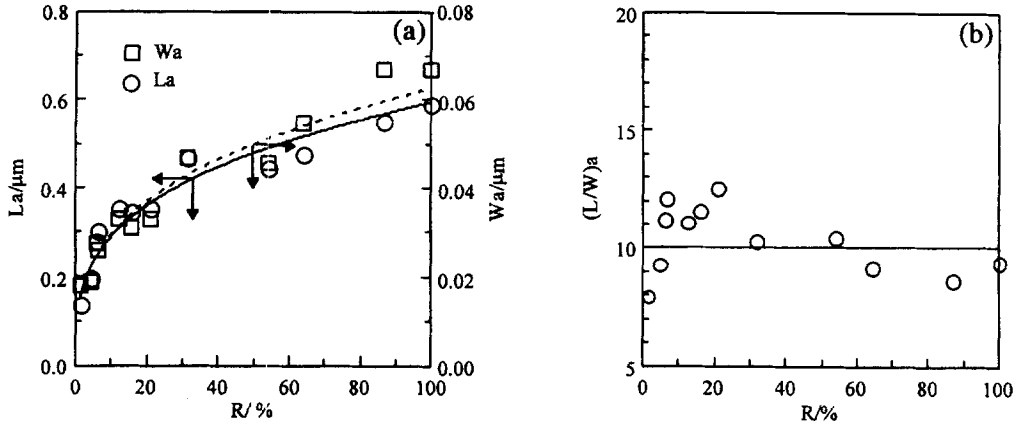

Fig. 5. Average length, width and aspect ratio vs conversion degree (test 2).

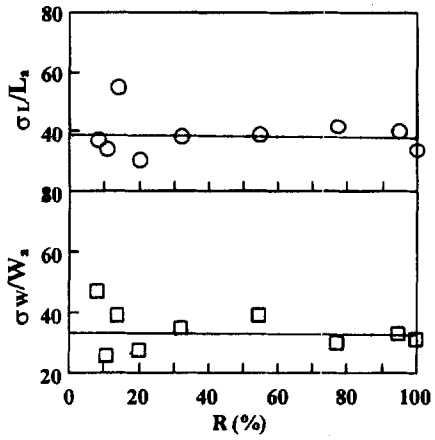

Fig. 6. Relative standard deviation of the length and width as a function of the degree of with conversion (test 1).

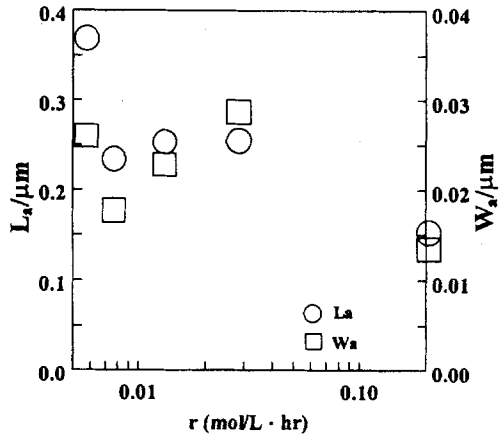

Fig. 7. Influence of the oxidation rate of the early period with $R \leq 20\%$ on the average length and width of the final crystal product.

Much nucleation occurs during the process in test 1 due to the starting concentration ($C_0 = 0.4$ mol l^{-1} in test 1 and $C_0 = 0.32$ mol l^{-1} in test 2) and the reaction rate.

Fig. 6 shows the relative standard deviation of the length (σ_L/L_a) width (σ_W/W_a) as a function of the degree of conversion in test 1. The relative standard deviation basically reflects the size distribution of the particles. Both σ_L/L_a and σ_W/W_a are roughly constant. Therefore, the size distribution does not change during the growth process of the grains.

3.3. *Influence of the oxidation rate in the early period*

According to the experiments, the oxidation rate in the early period plays an important role in the crystal growth process. Most of the nuclei form at the beginning of oxidation. In order to investigate the influence of the oxidation rate in the early period on the final products, we divided the oxidation process into two stages, i.e., the early period of oxidation at degrees of conversion of less than 20% and the latter oxidation stage at degrees of conversion of 20% to 100%. Experiments were carried out to analyse the size and aspect ratio of the final α-FeOOH product by changing the oxidation rate of the early stage and keeping the oxidation rate of the latter stage constant (0.08 mol l^{-1} h^{-1}, i.e., 3 h in the latter reaction). The experiments were carried out in a small-scale reactor with a volume of 1.5 l. The initial concentration of ferrous ions was 0.3 mol l^{-1}. The ratio of alkali to ferrous ions was 2.4, and the temperature was ~37–39°C. The reaction rate was controlled by adjusting the gas flux. Figs. 7 and 8 shows the influence of the oxidation rate of the early period on the average length, average width and aspect ratio of the final products.

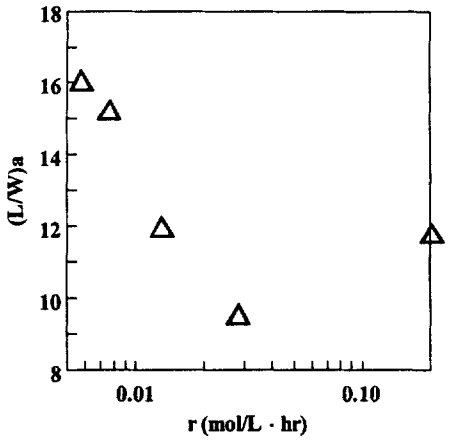

Fig. 8. Influence of the oxidation rate of the early period with $R \leq 20\%$ on the average value of the final crystal aspect ratio.

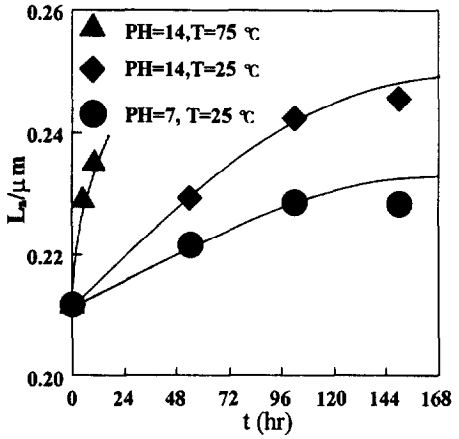

Fig. 9. Influence of aging time on the average length of the crystal for different aging methods.

Figs. 7 and 8 show that the size of the final product decreases with increasing oxidation rate, as does the aspect ratio. Consequently, a large number of small crystal seeds will be formed when the oxidation rate in the early period is comparatively fast, whereas at lower oxidation rates in the early period larger crystal seeds will be formed. Therefore it can be concluded that the aspect ratio of the final products is determined by the oxidation rate in the early period.

3.4. Aging effects

After completion of the reaction, the crystal grains were aged under certain conditions. It was found that the surface of the aged crystal grains becomes smoother, and the distribution of the grain size becomes more uniform. The crystal integrity is also improved. In the aging process, the smaller crystal grains are dissolved. Many flaws on the crystals with high potential energy disappear as a result of recrystallization. Fig. 9 shows that the average length of the crystal grains changes as a function of the aging time for different aging methods.

4. Conclusion

In this study, the nucleation and growth processes of α-FeOOH crystal grains, which are the intermediate products of magnetic recording media, were investigated under alkaline conditions.

The experiments shows that α-FeOOH crystals nucleate both on the surface of $Fe(OH)_2$ crystal grains and in the bulk liquid phase, depending on the local concentration of α-FeOOH molecules.

In the crystal growth process, the crystals grow in a similar manner and the size distribution is held roughly constant. The aspect ratio of the final α-FeOOH grains increases as the oxidation rate in the early period is decreased. The particle size changes as a result of aging under certain pH and temperature conditions.

5. Nomenclature

C_0	The initial concentration of Fe^{2+} (mol l^{-1})
k	Magnification of the crystal micrograph (dimensionless)
L	Crystal length (μm)
L_a	Average length of the crystals (μm)
M	Molecular weight (g mol^{-1})
N	Crystal number (dimensionless)
r	Reaction rate (mol l^{-1} h^{-1})
R	Conversion (%)
t	Time (h)
V	Average volume of the crystals (l)
W	Crystal width (μm)
W_a	Average width of the crystals (μm)
$(L/W)_a$	Average value of the crystal aspect ratios (dimensionless)

Greek letters

ρ	Goethite density (g cm^{-3})
σ_L	Standard deviation of the crystal length (μm)
σ_L/L_a	Relative standard deviation of the crystal length (dimensionless)
σ_W	Standard deviation of the crystal width (μm)
σ_W/W_a	Relative standard deviation of the crystal width (dimensionless)

References

[1] L.D. O'Connor, M.P. Dudukovic, P.A. Ramachandran, Ind. Eng. Chem. Res. 31 (1992) 2516–2524.
[2] W.Z. Feitknecht, Z. Elektrochem. 63 (1959) 34.
[3] T. Misawa, K. Hashimoto, S. Shimodaira, Corros. Sci. 14 (1974) 131.
[4] J.D. Bernal, D.R. Dasgupta, A.L. Mackay, Clay Min. Bull. 4 (1959) 15.
[5] E. Sada, H. Kumazawa, M. Aoyama, Chem. Eng. Commun. 71 (1988) 73–82.
[6] Y. Du, H. Lou, Magnetic Recording Media, Electric Industry Publishing House, 1992 (in Chinese).
[7] H. Gu, L. Hu, J. Chen, M. Chen, J. Eastern China Univ. Sci. Technol. 18 (1992) 467–484.
[8] A.J. Mahajan, D.J. Kirwan, AIChE J. 42 (1996) 1801–1814.